Dimethylpalladium(II) Complexes as Precursors for Chemical Vapor Deposition of Palladium

Zheng Yuan, Detong Jiang, S. J. Naftel, T.-K. Sham, and Richard J. Puddephatt*

Department of Chemistry, University of Western Ontario, London, Ontario, Canada N6A 5B7

Received June 28, 1994. Revised Manuscript Received August 22, 1994®

Dimethylpalladium(II) complexes, *cis*-[$PdMe_2(PR_3)_2$] (R = Me and Et) and [$PdMe_2$(tmeda)] (tmeda = *N,N,N′,N′*-tetramethylethylenediamine), were studied as precursors for low-temperature chemical vapor deposition (CVD) of thin films of palladium. All three precursors gave mirrorlike palladium films at substrate temperatures of 130–300 °C, using reduced pressure CVD. The films prepared by the simple thermal CVD process contained carbon impurities (*ca.* 10%) and a study by XANES and EXAFS indicates that the Pd–Pd distances are longer than in a pure palladium film. Typical film resistivities were 10^{-4} Ω cm for films of 0.5 μm thickness. For the phosphine-containing precursors, *cis*-[$PdMe_2(PR_3)_2$], CVD in the presence of hydrogen gave films which were essentially free of carbon impurities but which contained significant phosphorus impurity. Palladium films deposited from [$PdMe_2$(tmeda)] gave a much smoother surface than that from *cis*-[$PdMe_2(PMe_3)_2$] under the same CVD conditions. The thermal properties of the precursors were also studied in both the gas phase and condensed phase. Methane, ethane and ethylene were observed as volatile products of the CVD processes, and the product ratio was strongly dependent on the properties of the donor ligand. Methane was mainly formed by hydrogen reduction, ethane is the result of a simple intramolecular reductive elimination, and the significant amount of ethylene obtained on thermolysis of *cis*-[$PdMe_2(PEt_3)_2$] is derived from the Et_3P ligands.

Introduction

Palladium thin films are important materials in the electronics industry.[1] They are prepared commonly by physical vapor deposition (PVD), particularly by the ion sputtering technique. Deposition of palladium by photolysis of palladium(II) acetate or of [$Pd(N_3)_2(Ph_2PCH_2CH_2PPh_2)$] adsorbed on a surface is also useful for seeding further selective deposition of metals such as aluminum by thermal CVD.[2] By contrast, chemical vapor deposition (CVD) has received little attention, partly because PVD is superior to CVD in terms of quality of films and partly because the known CVD precursors are not ideal for commercial application.[1] However, the advantages of CVD over PVD, which include the ability to give conformal coating of complicated surfaces, rapid repair of expensive integrated circuits, and direct structure writing using a laser beam, suggest several potential applications if the process can be improved. Recently, it has been shown that CVD using allyl complexes [$Pd(\eta^3\text{-}CH_2CRCH_2)_2$] (R = H and CH_3), [$Pd(\eta^3\text{-}C_3H_5)Cp$] (Cp = η^5-cyclopentadienyl), and [$Pd(\eta^3\text{-}C_3H_5)$(hfac = hexafluoroacetylacetonato) as precursors can give palladium films of high purity.[2-5] Since the bis(η^3-allyl)palladium complexes are thermally unstable, the industrial potential of this type of precursor is limited. CVD of palladium from [$Pd(acac)_2$] and [$Pd(Cp)_2$] has been patented.[6] Although several volatile organoplatinum compounds have been studied as precursors for CVD,[1,7] many of the analogous palladium compounds are unsuitable either because they cannot be synthesized or because of their lower thermal stability. Clearly, there is still reason to search for new palladium precursors.

Several dimethylpalladium(II) compounds[8,9] are interesting candidates as CVD precursors since their syntheses are easy, and they have relatively high volatility and thermal stability. In this article we report low-temperature CVD of palladium films from a series of such dimethylpalladium(II) complexes, including a comparison of the products of thermolysis in the condensed and gas phases and analysis of film impurities. CVD of platinum from analogous organoplatinum complexes has been reported as has a preliminary conference report on this work.[7] This paper gives a full account of the CVD of palladium from dimethylpalladium precursors, including the effects of CVD conditions and supporting ligands on the purity of the palladium films. The prepared films were characterized by XPS,

® Abstract published in *Advance ACS Abstracts,* October 1, 1994.

(1) (a) Gurney, P. D.; Seymour, R. J. In *Chemistry of the Platinum Group Metals,* Hartley, F. R., Ed.; Elsevier: Amsterdam, 1991; Chapter 17, p 594. (b) Gliem, R.; Schlamp, G. *Metall. Technol.* **1987,** *41,* 34.

(2) (a) Estrom, H.; Kogelschatz, U. *Appl. Surf. Sci.* **1990,** *46,* 158. (b) Zhang, Y.; Stuke, M. *Appl. Surf. Sci.* **1990,** *46,* 153. (c) Lehmann, O.; Stuke, M. *Appl. Phys. Lett.* **1992,** *61,* 2027. (d) Ho, T. W. H.; Blair, S. L.; Hill, R. H.; Bickley, D. G. *J. Photochem. Photobiol.* **1992,** *69,* 229.

(3) (a) Gozum, J. E.; Pollina, D. M.; Jensen, J. A.; Girolami, G. S. *J. Am. Chem. Soc.* **1988,** *110,* 2688. (b) Lin, W.; Warren, T. H.; Nuzzo, R. G.; Girolami, G. S. *J. Am. Chem. Soc.* **1993,** *115,* 11644. (c) Lin, W.; Wilson, S. R.; Girolami, G. S. *Inorg. Chem.* **1994,** *33,* 2265.

(4) (a) Thomas, R. R.; Park, J. M. *J. Electrochem. Soc.* **1989,** *136,* 1661. (b) Kim, Y. G.; Bialy, S.; Stauf, G. T.; Miller, R. W.; Spencer, J. T.; Dowben, P. A.; Datta, S. *J. Micromech. Eng.* **1991,** *1,* 42. (c) Feurer, E.; Suhr, H. *Thin Solid Films,* **1988,** *157,* 81.

(5) Yuan, Z.; Puddephatt, R. J. *Adv. Mater.* **1994,** *6,* 51.

(6) Kudo, T.; Yamaguchi, A. Japanese Patent JP 62207868, 1987.

(7) (a) Xue, Z. L.; Thridandam, H.; Kaesz, H. D.; Hicks, R. F. *Chem. Mater.* **1992,** *4,* 162. (b) Kumar, R.; Roy, S.; Rashidi, M.; Puddephatt, R. J. *Polyhedron* **1989,** *8,* 551. (c) Yuan, Z.; Puddephatt, R. J. *Abstr. Nat. ACS Conference*; Chicago, 1993, Paper INOR 26.

(8) (a) Calvin, G.; Coates, G. E. *J. Chem. Soc.* **1960,** 2008. (b) Tooze, R.; Chiu, K. K.; Wilkinson, G. *Polyhedron* **1984,** *3,* 1025.

(9) de Graaf, W.; Boersma, J.; Smeets, W. J. J.; Spek, A. L.; van Koten, G. *Organometallics* **1989,** *8,* 2907.

0897-4756/94/2806-2151$04.50/0

SEM, and conductivity. Additional information on the local structure Pd in the films was provided by XAFS studies. Some of the difficulties of obtaining pure palladium films from these precursors can be understood in terms of the mechanisms of thermal decomposition involved in the CVD process.

Experimental Section

All reactions involving lithium reagents and phosphine compounds were carried out using standard drybox or Schlenk techniques under a nitrogen atmosphere. Diethyl ether and benzene were distilled under nitrogen over sodium. ^1H, ^{13}C, and ^{31}P NMR spectra were recorded by using a Varian XL-300 instrument. GC-MS spectra were recorded by using a Varian MAT 311A instrument. Gas-phase infrared spectra were obtained by using a Perkin-Elmer System 2000 FT-IR spectrometer.

Precursor Synthesis. *cis*-[$PdMe_2(PEt_3)_2$] was prepared by using a literature procedure, in which [$PdBr_2(PEt_3)_2$] was prepared by reaction of [$PdCl_2(PEt_3)_2$] with LiBr in acetone and then converted to *cis*-[$PdMe_2(PEt_3)_2$] by methylation with $LiCH_3$.[8] By using the same method, *cis*-[$PdMe_2(PMe_3)_2$] was also prepared in 62% yield.[8] [$PdMe_2$(tmeda)] and [$Pd(CD_3)_2$(tmeda)] were prepared using a recently published approach,[9] by reaction of $PdCl_2$ with tmeda in CH_3CN to give [$PdCl_2$(tmeda)], followed by methylation with $LiCH_3$ and $LiCD_3$, respectively. [$PdMe_2$(eda)] (eda = ethylenediamine) was prepared by substitution of tmeda in [$PdMe_2$(tmeda)] with a large excess of ethylenediamine.[9]

[$PdMe_2$(teeda)]. To a solution of [$PdCl_2(NCC_6H_5)_2$] (0.93 g, 2.4 mmol) in benzene (20 mL), was added *N,N,N',N'*-tetraethylethylenediamine (0.45 g, 2.4 mmol) at room temperature. After removal of the solvent, a yellow product (0.8 g), [$PdCl_2$(teeda)], was obtained. An ether solution of 1.4 M $LiCH_3$ (3.15 mL, 4.4 mmol) was added to the [$PdCl_2$(teeda)] (0.77 g) in Et_2O (20 mL). After extraction with water, the ether solution was dried by $MgSO_4$ and the ether was removed under reduced pressure to give a pale-yellow crystalline product (yield 0.33 g, 49%). Mp ~110 °C (dec) (it decomposed gradually at room temperature). NMR in C_6D_6 δ (^1H) 2.2–2.3 and 2.5–2.6 (m, CH_2CH_3, 8H), 1.89 (s, CH_2CH_2, 4H), 1.07 (t, 7.2 Hz, CH_2CH_3, 12H), 0.48 (s, $PdCH_3$, 6H); $\delta(^{13}C)$ = 50.5 (CH_2CH_3), 49.3 (H_2CH_2), 10.9 (CH_2CH_3), −6.9 ($PdCH_3$).

Thermal CVD experiments were conducted by using a Pyrex vertical cold-wall reactor at reduced pressure with dynamic pumping, unless otherwise specified. A sidearm was present to enable introduction of a carrier gas. The substrate, which was usually a glass plate, was heated by a temperature-controlled heating rod. As [$PdMe_2$(tmeda)] reacted with H_2 at room temperature, CVD was carried out using a hot-wall CVD reactor with two gas inlets, one for a N_2 carrier gas and the other for introducing H_2 at the substrate.

The films produced by CVD were analyzed by XPS and SEM equipped with EDX (energy-dispersive X-ray analysis). XPS spectra were obtained by using a SSL SSX-100 small-spot XPS surface-analysis instrument with a monochromatized Mg Kα X-ray source (1253.6 eV). All Pd thin films reported in this paper were sputtered with argon until no further change of element composition occurred (normally, 1 min at 4 keV), before recording the analysis. Analytical data are given in units of atom percent in Table 1. SEM micrographs of Pd films were taken by using an ISL DS-130 scanning electron microscope. Film resistivities were measured by using a Veeco FPP 5000 4-point probe apparatus.

The Pd L-edge XAFS spectra were obtained on the double-crystal monochromator (DCM) beamline, equipped with InSb(111) crystals,[10] of the Canadian Synchrotron Radiation Facility (CSRF) at the Synchrotron Radiation Centre (SRC), University of Wisconsin—Madison. XAFS were recorded in the total electron yield mode in a vacuum chamber in which the specimen current of the films was recorded as a function of photon energy. The Pd K-edge XAFS spectra were obtained on the C2 station of the Cornell High Energy Synchrotron Source (CHESS) using a He gas amplified total electron yield detector for the CVD films and using transmission mode for the Pd metal reference. The incoming beam was monitored with an Ar-filled ionization chamber.

Thermolysis of precursors under N_2 was monitored by thermogravimetric analysis, TGA. Volatile thermal decomposition products from decomposition in both the condensed phase and the vapor phase were determined by FTIR, GC, and GC-MS. Quantitative analysis of gas components was performed by using a Varian 3400 gas chromatograph with a packed column and a flame ionization detector (FID) set at 250 °C. The injection temperature was 200 °C, and the oven temperature was 30 °C. The peak areas of GC spectra were calibrated using commercial standard gas references; total gas yields accounted for at least 80% of the methylpalladium groups, and relative yields are given in Table 2. All peaks were fully resolved under our experimental conditions. C_2D_6 gave an ion pattern of *m/e* at 28[$M - 4D)^+$, 18], 30[$(M - 3D)^+$, 26], 32[$(M - 2D)^+$, 100], 34[$(M - D)^+$, 15] and 36(M^+, 19), with the expected peak intensity distribution predicted from the spectrum of C_2H_6. The mass spectrum of the ethane obtained from the mixture of [$PdMe_2$(tmeda)] and [$Pd(CD_3)_2$(tmeda)] was as predicted for the sum of mass spectra of C_2H_6 and C_2D_6. In particular, using the peak of *m/e* at 26 from C_2H_6 and the peak of *m/e* at 36 from C_2D_6 as references, it is found that the measured peak height of *m/e* at 30 is almost the same as the calculated result from the sum of M^+ of C_2H_6 and $[M - 3D]^+$ of C_2D_6. The difference is within the experimental error (±5%). If the product from crossover coupling, namely, CH_3CD_3, were

Table 1. Deposition Conditions and Film Properties for CVD of Pd from $PdMe_2L_2$

precursor	pressure carrier gas, Torr	substrate temp, °C	XPS, atom % Pd	C	P
$PdMe_2(PMe_3)_2$	10^{-3}	200	88	12	0
$PdMe_2(PMe_3)_2$	1/H_2	150	89	11	0
$PdMe_2(PMe_3)_2$	1/H_2	200	88	0	12
$PdMe_2(PEt_3)_2$	10^{-3}	220	91	9	0
$PdMe_2(PEt_3)_2$	10^{-3}	300	92	8	0
$PdMe_2(PEt_3)_2$	1/H_2	200	90	0	10
$PdMe_2$(tmeda)	10^{-3}	150	90	10	0
$PdMe_2$(tmeda)	10^{-3}	230	87	13	0
$PdMe_2$(tmeda)	$10^{-1}/H_2$, N_2	130	89	11	0

Table 2. Gaseous Products from CVD and from Condensed-Phase Pyrolysis of $PdMe_2L_2$[a,b]

precursor	conditions[a] atmosphere	temp, °C	GC anal. CH_4	CH_3CH_3	$CH_2{=}CH_2$
$PdMe_2(PMe_3)_2$	CVD	150	54	46	[c]
$PdMe_2(PMe_3)_2$	CVD/H_2	150	93	7	[c]
$PdMe_2(PMe_3)_2$	solid-state 1 atm N_2	140	56	44	[c]
$PdMe_2(PMe_3)_2$	solid-state 1 atm H_2	70	99	1	[c]
$PdMe_2(PEt_3)_2$	CVD	150	44	34	22
$PdMe_2(PEt_3)_2$	CVD	200	27	32	39
$PdMe_2(PEt_3)_2$	CVD/PEt_3	150	47	25	28
$PdMe_2(PEt_3)_2$	CVD/H_2	150	89	10	1
$PdMe_2(PEt_3)_2$	liquid, PEt_3 1 atm N_2	140	9	90	1
$PdMe_2(PEt_3)_2$	liquid 1 atm N_2	140	11	80	9
$PdMe_2(PEt_3)_2$	liquid 1 atm H_2	70	93	7	[c]
$PdMe_2$(tmeda)	CVD	150	74	21	5
$PdMe_2$(tmeda)	solid state 1 atm N_2	150	74	20	6

[a] CVD was conducted under partial vacuum. [b] Analyses were calibrated by using standard gas mixtures. [c] Trace of $CH_2{=}CH_2$ was observed.

(10) Yang, B. X.; Middleton, F.; Olsson B. G.; Bancroft G. M.; Chen J. M.; Sham T. K.; Tan K. H.; Wallace D. J. *Nucl. Instrum. Methods A* **1990**, *316*, 422.

formed from the mixed precursors, the highest ion peak $[M - HD]^+$ at *m/e* 30 should have significantly greater intensity.

Results and Discussion

CVD Experiment. $[PdMe_2(eda)]$ and $[PdMe_2(teeda)]$ decomposed before subliming in vacuo, so that they were not suitable for the CVD process under our experimental conditions. Therefore, the current studies were focused on *cis*-$[PdMe_2(PMe_3)_2]$, *cis*-$[PdMe_2(PEt_3)_2]$, and $[PdMe_2(tmeda)]$. These three precursors were warmed to 40–50 °C in all CVD experiments to provide sufficient vapor pressure for CVD. Deposition pressure and temperature for different experiments are given in Table 1, along with results of XPS analysis of the palladium thin films produced. Without a carrier gas, depositions were conducted at a pressure of 10^{-3} Torr. In these cases, the lowest deposition temperature was 200 °C for *cis*-$[PdMe_2(PMe_3)_2]$, 220 °C for *cis*-$[PdMe_2(PEt_3)_2]$, and 150 °C for $[PdMe_2(tmeda)]$. In the presence of H_2 (~1 Torr pressure), the deposition of palladium from *cis*-$[PdMe_2(PMe_3)_2]$ and *cis*-$[PdMe_2(PEt_3)_2]$ could be carried out at substrate temperature ca. 20–50 °C lower than those without H_2 gas. Under optimum conditions, the film growth rates were dependent on the precursor volatility; with the precursor reservoir at 45 °C, the film growth rate was 0.9 $\mu m\ h^{-1}$ for $[PdMe_2(tmeda)]$ and 0.2 $\mu m\ h^{-1}$ for *cis*-$[PdMe_2(PMe_3)_2]$ or *cis*-$[PdMe_2(PEt_3)_2]$.

CVD of palladium from $[PdMe_2(tmeda)]$ in the presence of hydrogen was unsuccessful using the vertical reactor since hydrogen led to decomposition of the precursor before volatilization. Thus a new reactor, as described in the Experimental Section, was designed for this CVD experiment. Nitrogen was used as carrier gas and hydrogen was introduced at the substrate; the flow rate of N_2 was higher than that of H_2 to minimize back diffusion of hydrogen. Even so, much care was needed to obtain palladium films in the presence of hydrogen. Optionally, the total pressure was 0.1 Torr, maintained by dynamic pumping, the precursor was heated no higher than 50 °C, and the substrate was heated to 130 °C.

Composition and Nature of the Palladium Films. All palladium films prepared from the dimethylpalladium precursors were shiny and mirrorlike. They gave good adhesion to silicon but poorer adhesion to glass substrates as tested by scratch or adhesive-tape tests. EDX and XPS were used to analyze the films. Since EDX is less reliable for determining carbon contamination, the analyses of palladium films obtained by XPS are given (Table 1). A typical XPS spectrum of the palladium film prepared by thermal CVD of a dimethylpalladium complex is illustrated in Figure 1. The peak due to Pd $3d_{5/2}$ was at 335.0 eV, which is slightly lower than the literature value (335.1–335.4 eV).[11] The palladium films were amorphous. In the absence of hydrogen carrier gas, the films contained significant carbon impurities. The peak in the XPS spectrum due to C(1s) was at 284.2 eV, which is in the range expected for graphite. The carbon content was in the range 8–13 atom % for CVD from *cis*-$[PdMe_2(PMe_3)_2]$, *cis*-$[PdMe_2(PEt_3)_2]$, and $[PdMe_2(tmeda)]$. The carbon contamination varied only little with the substrate temperature during the deposition. For the dimethylbis(trialkylphosphine)palladium(II) complexes, the level of carbon contamination decreased to effectively zero when the deposition was carried out using a hydrogen carrier gas but phosphine contamination occurred instead, as was indicated by the XPS analysis (Table 1). Phosphorus was analyzed by the peaks due to P(2s) at 188.5 eV and P(2p) at 130.9 eV. This result suggested that, in the presence of hydrogen, CVD from $[PdMe_2(tmeda)]$, which contains no phosphorus, should give pure palladium films. Unfortunately, as discussed earlier, CVD of palladium in the presence of hydrogen was difficult using the precursor $[PdMe_2(tmeda)]$ due to hydrogenolysis before volatilization. Under the best operating conditions, the carbon contamination of the film was 11 atom %, unchanged from CVD in the absence of hydrogen. If higher hydrogen pressures were used, the precursor decomposed before volatilization.

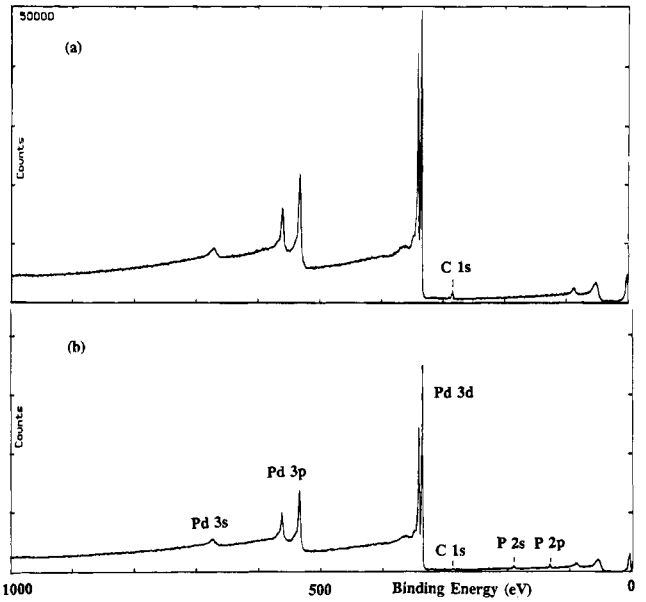

Figure 1. XPS of Pd films: (a) from $[PdMe_2(tmeda)]$; (b) from $[PdMe_2(PMe_3)_2]$ with H_2.

Micrographs obtained by SEM of the palladium films prepared from *cis*-$[PdMe_2(PMe_3)_2]$ and $[PdMe_2(tmeda)]$ are shown in Figure 2. Although both films were deposited at the same temperature and have almost the same composition, the film micrographs are quite different. The particle size of the film from *cis*-$[PdMe_2(PMe_3)_2]$ is ca. 0.2 μm which is at least 1 order of magnitude larger than that from $[PdMe_2(tmeda)]$.

The resistivities of representative palladium films were measured by using the four-point probe method. Typical values were as follows: for the precursor $[PdMe_2(tmeda)]$, $1.1 \times 10^{-4}\ \Omega$ cm (thickness 0.8 μm); $[PdMe_2(PMe_3)_2]$, $6.9 \times 10^{-5}\ \Omega$ cm (thickness 0.1 μm); $[PdMe_2(PEt_3)_2]$, $5.8 \times 10^{-5}\ \Omega$ cm (thickness 0.4 μm). For comparison, bulk palladium has a resistivity of $1.1 \times 10^{-5}\ \Omega$ cm, so the film resistivities were 5–10 times greater than for pure bulk palladium. This may be attributed to the presence of carbon impurities and is consistent with structural observations discussed below.

X-ray Absorption Fine Structure Spectroscopy (XAFS) Analysis. To study the nature of carbon contaminations in the Pd films, XAFS analyses were conducted on the palladium films deposited by thermal CVD from *cis*-$[PdMe_2(PMe_3)_2]$ and $[PdMe_2(tmeda)]$.

(11) *Handbook of X-ray Photoelectron Spectroscopy*; Perkin-Elmer Corp., 1992.

(a)

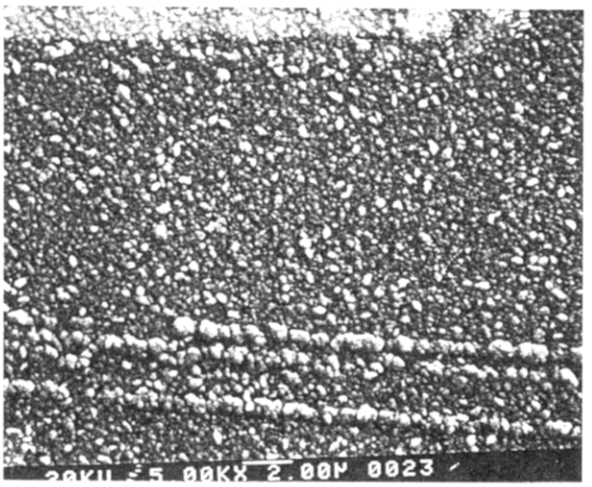

(b)

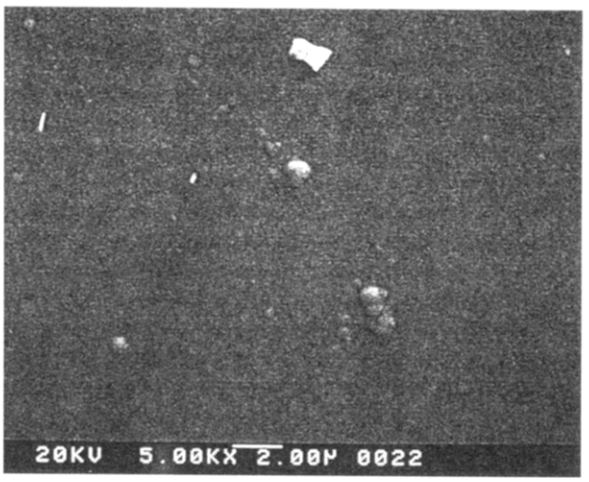

(c)

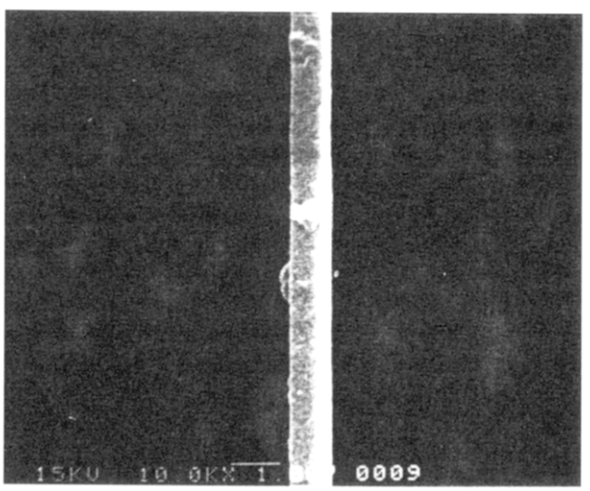

Figure 2. SEM of Pd films: (a) from [$PdMe_2(PMe_3)_2$]; (b) from [$PdMe_2$(tmeda)]; (c) cross section from [$PdMe_2$(tmeda)].

Each of these films contained *ca.* 10% carbon impurity as determined by XPS analysis.

XAFS spectra were recorded in both the near-edge region (~50 eV above the threshold) and the extended X-ray absorption fine structure (EXAFS) region (up to as much as 1000 eV above the threshold); modern theory can now treat the whole region as one satisfactorily.[12]

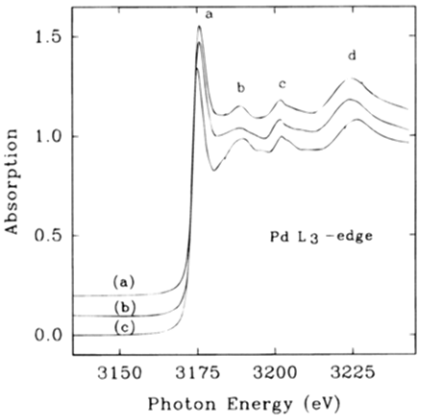

Figure 3. PdL_3 edge near edge structure for (a) Pd CVD film A [$PdMe_2(PMe_3)_2$], (b) film B [$PdMe_2$(tmeda)], (c) Pd metal reference; all spectra have been normalized to the edge jump and shifted vertically for clarity.

Figure 3 shows the X-ray absorption near edge structure (XANES) of the Pd L_3 edge for Pd metal, Pd CVD film A [$PdMe_2(PMe_3)_2$ at 200 °C, 12% C impurity], and film B [$PdMe_2$(tmeda) at 150 °C, 10% C impurity]. At first glance, all spectra exhibit very similar spectral features. The Pd L_3 edge XANES shows an intense whiteline[13] at the threshold (peak a) followed by three sets of resonances (b–d) within the first 50 eV beyond the whiteline. These features have been well characterized.[14,15]

The result of Figure 3 indicates that the Pd film prepared by CVD differs from Pd metal in at least two ways. First, the less pronounced resonances b and c which are sensitive to the band structure[14] of Pd metal indicate that there is some degradation in the long-range order; similar conclusion can be arrived at based on the cluster model[15] since it has been recognized that at least three to four shells of neighboring atoms in a cluster constructed according to the lattice structure are required to reproduce a near-edge structure that resembles that of bulk metal. Second, the shift of the energy position of the resonances b–d toward the threshold indicates a longer Pd–Pd bond in the CVD film than in the pure metal. These results are confirmed with K-edge XAFS measurements presented below.

Figure 4 shows the Pd K-edge XAFS of Pd metal and the CVD films A and B. It is immediately apparent that both CVD films again exhibit XAFS very similar to that of the Pd metal except that the oscillations are compressed toward the threshold with a less-pronounced amplitude. Close observation reveals two interesting features: first, there exhibits a progressively increasing mismatch of the oscillation maxima between the CVD films and Pd metal with the CVD Pd shifted toward the threshold, similar to that observed in the L_3 edge; second, the amplitude of the oscillations is considerably smaller in the EXAFS of the CVD films than that of

(12) Proceedings of the 7th Int. Conf. on XAFS, Kobe, Japan, Aug 1992, *Jpn J. Appl. Phys. Suppl.* **1993**, 32–2.
(13) Sham T. K. *Phys. Rev. B* **1985**, *13*, 1903.
(14) Muller J. E.; Jepsen O.; Wilkins J. W. *Solid State Commun.* **1982**, *42*, 365.
(15) Bianconi, A. Garcia, J.; Benfatto, M. Synchrotron Radiation in Chemistry and Biology I. *Top. Curr. Chem.* **1986**, *145*.

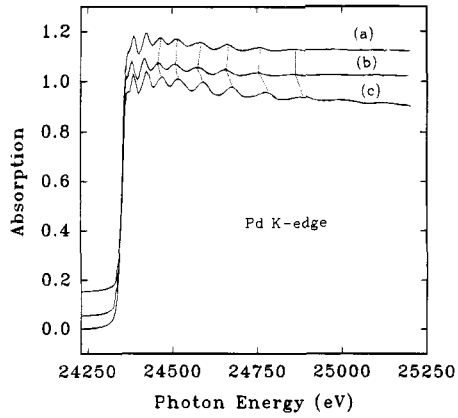

Figure 4. Pd K-edge XAFS of (a) CVD film A, (b) CVD film B, and (c) Pd metal reference. The mismatch in energy position of the oscillations is noted.

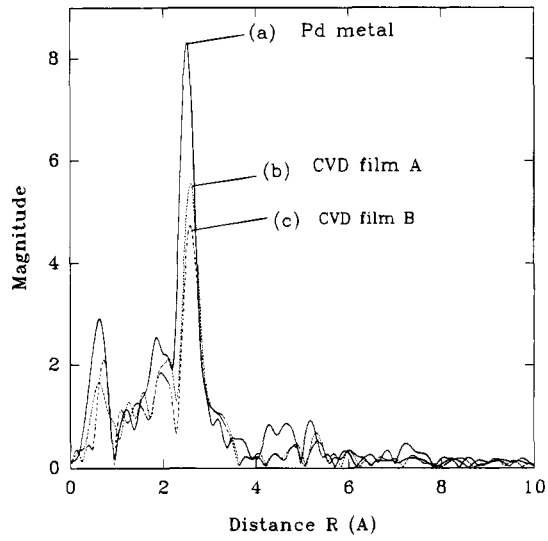

Figure 5. Fourier transform of the EXAFS derived from Figure 2 with k weighting and a data length of ~4–14 Å^{-1}. The most intense peak corresponds to the Pd–Pd bond length.

the pure metal. The compressed and somewhat diminished EXAFS oscillations seen in the CVD Pd films indicate a degradation in the long range order with relaxed Pd–Pd bonds (longer bond length) and larger Debye–Waller factor than that of the Pd metal; the significant reduction in amplitude suggests that the average coordination number is also smaller as the result of a bigger surface atom to bulk atom ratio in these films than in pure Pd metal.

The above described changes are best seen in the Fourier transforms (FT) of the normalized EXAFS shown in Figure 5. The most intense peak in the radial distribution function corresponds to the first shell Pd–Pd interatomic distance (2.75 Å) in Pd metal.[13] It can be seen that the corresponding Pd–Pd bond length in the CVD films is noticeably longer than that of Pd metal. A fit using the phase difference method produces a bond length difference of 0.10 Å, indicating that the CVD Pd–Pd bond has relaxed by 3.6% compared to that of pure metal.

The reduction in EXAFS amplitude may also be due to the presence of Pd–C bonds since XPS indicates that there is as much as 10% graphite-type carbon on the surface. In Figure 5 there is some indication that there may a small Pd–C component in the ~2 Å region, but its contribution to the overall EXAFS is small as is seen in the first few hundred electronvolt region of the absorption spectra where strong beating due to the presence of another sinusoidal wave of different phase (presumably due to the Pd–C pair) is not evident.

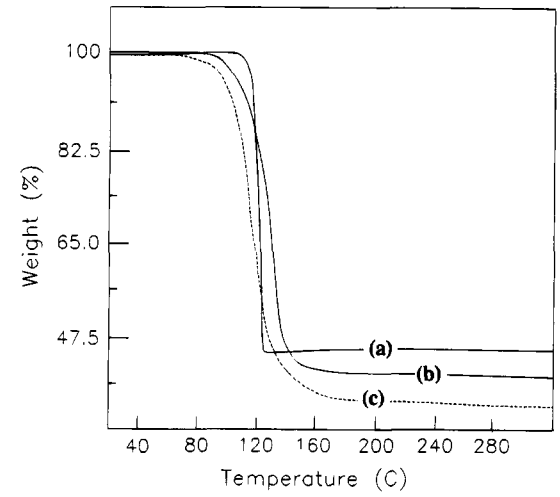

Figure 6. TGA traces of (a) [$PdMe_2$(tmeda)], (b) [$PdMe_2(PMe_3)_2$], and (c) [$PdMe_2(PEt_3)_2$]. Note the very narrow temperature range for decomposition of [$PdMe_2$(tmeda)].

From these results it is no doubt that the Pd CVD films reported here exhibit unusual structural properties in that they have longer Pd–Pd bonds than that of the pure Pd metal. If these films are composed of aggregates of small Pd clusters, this observation is in contrast to conventional wisdom[16,17] which believes that the interatomic distance in small clusters often contracts relative to the bulk value.[17] This apparent discrepancy could be due to either the effect of strong Pd–support interaction or the incorporation of C in the Pd films. More detailed studies are now in progress to address these issues.

TGA Analysis. Thermogravimetric analysis (TGA) was used to monitor decomposition of *cis*-[$PdMe_2(PMe_3)_2$], *cis*-[$PdMe_2(PEt_3)_2$], and [$PdMe_2$(tmeda)]. All of these three compounds showed a simple one-step decomposition under a nitrogen atmosphere. The measured weight loss was 60–63% (70–360 °C) for *cis*-[$PdMe_2(PMe_3)_2$], 65–68% (40–370 °C) for *cis*-[$PdMe_2(PEt_3)_2$], and 56–57% (70–350 °C) for [$PdMe_2$(tmeda)], compared to the theoretical values of 63.1%, 71.4%, and 57.9% in terms of the percentage of the Pd metal in the corresponding precursors. The range of decomposition temperature of [$PdMe_2$(tmeda)] is particularly narrow (see Figure 6). These data are again consistent with the film analyses, which show that residue is largely metallic palladium with some carbon.

GC and GC-MS Analysis. To obtain a more complete picture of the CVD process and, particularly, to try to understand the origin of the carbon contamination of the palladium films, a study of the organic products of CVD was carried. The gaseous products formed by thermal decomposition of the precursors in the gas phase were compared to those from decomposition in the condensed (solid or liquid) phase. Volatile decomposition products were analyzed by GC and GC-MS.

(16) Hamilton, J. F.; Logel, P. C. *Thin Solid Films* **1973**, *16*, 49.
(17) Apai, G.; Hamilton, J. F.; Stohr; A. Thompson *Phys. Rev. Lett.* **1979**, *43*, 165.

Data from quantitative GC analysis of gas-phase products obtained under different conditions are listed in Table 2. Most of the supporting ligand was accounted for as the free ligand PR_3 or tmeda (>90%), and so Table 2 shows only the products arising largely from the dimethylpalladium groups.

Decomposition of *cis*-[$PdMe_2(PMe_3)_2$] in the gas phase and the solid state gave similar amounts of methane (ca. 55%) and ethane (ca. 45%). In the presence of H_2, the proportion of methane increased to over 90% in both states and the decomposition temperature was decreased substantially.

Unlike *cis*-[$PdMe_2(PMe_3)_2$], the decomposition in the condensed (liquid) phase and vapor phase of *cis*-[$PdMe_2(PEt_3)_2$] gave very different ratios of volatile products. In the liquid phase (MP 45 °C), the products were ethane (80%), methane (11%), and ethylene (9%). Calvin and Coates reported that thermolysis of *cis*-[$PdMe_2(PEt_3)_2$] at 100 °C in a sealed tube gave a mixture of ethane (92%) and ethylene (8%) with only a trace of methane.[8] When decomposition of the precursor was carried out in the vapor phase, both methane and ethylene became very significant products (Table 2). The methane/ethane ratio was higher early in the reaction (especially in the first 2–3 min) and then decreased with time. The percentage of ethylene increased with increasing decomposition temperature. Under CVD conditions, the thermolysis of *cis*-[$PdMe_2(PEt_3)_2$] in the presence of free PEt_3 led to an increase in methane yield relative to ethane and ethylene but, in the liquid phase, ethane formation was favored and only traces of ethylene were formed. In the presence of hydrogen, methane became the major product in both liquid- and vapor-phase reactions.

The thermal decomposition of [$PdMe_2$(tmeda)] in the solid state and in solution has been reported recently. A mixture of methane and ethane in a 3/1 ratio with varying small amounts of other C_2 hydrocarbons was observed.[9] The yields of volatile products from the gas-phase and solid-state decompositions were essentially the same in our studies, namely, 74% methane, 20% ethane, and 6% ethylene, in reasonable agreement with the literature values.[9]

The gas-phase decomposition [$PdCD_3)_2$(tmeda)] was conducted, and the isotopic compositions of the main volatile decomposition products, methane and ethane, were analyzed by using GC/MS. In several experiments carried out in similar conditions, the methane contained both CD_3H and CD_4, with the ranges CD_3H 90–97% and CD_4 3–10%. Obviously, methane is formed mainly by combination of a CD_3 group with a proton source (tmeda or adventitious hydrogen) rather than from the neighboring CD_3 group.

The ethane from gas-phase thermolysis of [$Pd(CD_3)_2$(tmeda)] was C_2D_6, as expected from the coupling of the methylpalladium groups. Mass spectral analysis of the ethane formed by gas-phase thermolysis of a 1:1 mixture of [$PdMe_2$(tmeda)] and [$Pd(CD_3)_2$(tmeda)] showed formation of C_2H_6 and C_2D_6 only with no CH_3CD_3 (analysis 0 ± 5%). This shows clearly that ethane is formed by intramolecular coupling of methylpalladium groups and not by intermolecular reaction. It has been reported previously that much CH_3CD_3 is formed on thermolysis of a solution containing a mixture of *trans*-[$PdMe_2(PMePH_2)_2$] and *cis*-[$Pd(CD_3)_2(PMePh_2)_2$], but no cross-over product was formed from similar decomposition of a mixture of *cis*-[$PdMe_2(PMePh_2)_2$] and *cis*-[$Pd(CD_3)_2(PMePh_2)_2$].[18]

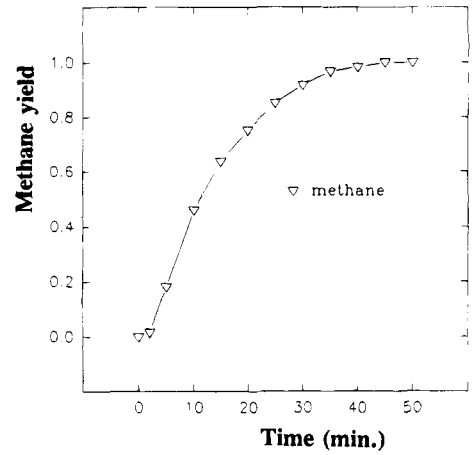

Figure 7. Growth of the peak due to ν(CH) of CH_4 at 3017 cm^{-1} during the thermolysis of [$PdMe_2(PEt_3)_2$] at 150 °C in an FTIR gas cell.

Gas-Phase FT-IR Studies. Complementary information on the gas-phase products was obtained by monitoring the gas-phase thermolyses of dimethylpalladium complexes by FTIR, using a heated evacuated gas cell. The formation of methane was easily monitored by growth of the band due to ν(C–H) at 3017 cm^{-1}, but bands due to ethane and ethylene were partly obscured by ligand bands. The growth of the methane peak in a typical experiment, in which the evacuated IR cell containing *cis*-[$PdMe_2(PEt_3)_2$] was heated to 150 °C, is shown in Figure 7. Qualitatively, after a brief induction period, the formation of methane was faster than ethane initially, confirming the observation made by GC, although ethane was the major product overall. Similar observations were made for decomposition of *cis*-[$PdMe_2(PMe_3)_2$].

Decomposition Pathways. Decomposition pathways for the thermolysis of dimethylpalladium complexes in solution have been studied extensively, but there has been very little research on gas-phase decomposition which is central to understanding the CVD process.[8,9,18] In this work, similarities between the volatile products of gas-phase and condensed-phase thermal decomposition were observed in many cases. For instance, *cis*-[$PdMe_2(PMe_3)_2$], when decomposed in the vapor or in the solid state, gave essentially the same ratio of methane to ethane. So did [$PdMe_2$(tmeda)], producing methane and ethane, as well as ethylene. The ratio of volatile products was influenced strongly by the properties of the donor ligands L in [$PdMe_2L_2$]. Decomposition of methylpalladium compound with the stronger donor ligand tmeda gives less ethane than with phosphine ligands. It has been shown that thermolysis of [$Pd(CD_3)_2$(tmeda)] in the solid state gave a ratio of CD_4/CD_3H = 3.5/1, while in benzene solution it gave CD_4/CD_3H = 0.5/1. Thermolysis of [$PdMe_2$(tmeda)] in C_6D_6 gave CH_4/CH_3D = 5–8/1 which, by comparison with the previous data, indciates that there is a large isotope effect for the H (or D) abstraction step.[9] In the gas-phase thermolysis of [$Pd(CD_3)_2$(tmeda)], the ratio

(18) Ozawa, F.; Ito, T.; Nakamura, Y.; Yamamoto, A. *Bull. Chem. Soc. Jpn.* **1981**, *54*, 1868.

of $CD_4/CD_3H = 0.03-0.1/1$. There are dramatic differences, with the relative yield of CD_4/CD_3H on thermolysis of $[Pd(CD_3)_2(tmeda)]$ following the series solid state > solution phase > gas phase. In solution, there may be competition between abstraction from the second methylpalladium group, giving CD_4, from the tmeda ligand or from the solvent, both giving CD_3H. The solvent abstraction accounts easily for the higher yield of CD_3H compared to the solid state thermolysis.[9] It is less obvious why the CD_3H yield is even higher for the gas-phase thermolysis. We suggest that since the concentration of $[Pd(CD_3)_2(tmeda)]$ in the gas phase is very low, there are sufficient hydroxyl hydrogen atoms on the surface of the glass vessel to react with the CD_3-Pd groups to form CD_3H. Our previous studies on thermolysis of *cis*-$[PtMe_2(CNME)_2]$ has shown that methane was formed by combination of a methylplatinum group with hydrogen atom from the cell wall.[19] This proposed reaction with surface hydroxyl groups can be represented by eq 1,in which *SiOH represents a

$$*SiOH + [PdMe_2L_2] \rightarrow *SiOPdMeL_2 + CH_4 \quad (1)$$

surface hydroxyl group. This step appears particularly important in the early stages of reaction and may be responsible, after further thermolysis steps, for the formation of the initial palladium clusters needed to act as centers for adsorption and decomposition of other precursor molecules.

The formation of ethane by reductive elimination has been established in solution thermolysis of complexes $[PdMe_2(PR_3)_2]$ by several previous studies.[18,20,21] The formation of ethylene is more complicated. Among the three dimethylpalladium compounds, the ethylene level is in the order of *cis*-$[PdMe_2(PEt_3)_2]$ (20–40%) > $[PdMe_2$-(tmeda)] (5–6%) > *cis*-$[PdMe_2(PMe_3)_2]$ (trace). The difference between the complexes with PMe_3 and PEt_3 ligands is dramatic and strongly suggests that the ethylphosphorus groups are involved in ethylene formation in the thermolysis of *cis*-$[PdMe_2(PEt_3)_2]$.

The observation that thermolysis of the complexes *cis*-$[PdMe_2(PR_3)_2]$ in the presence of hydrogen leads to phosphorus impurity in the palladium films was unexpected. It seems that hydrogen must promote P–C bond cleavage to give initially phosphido groups, which are not easily desorbed from the surface. Eventually, complete hydrogenation of the alkylphosphorus groups gives CH_4 from PMe_3 and C_2H_6 from PEt_3 and leaves phosphorus impurities only. Girolami and co-workers have very recently suggested that P–C bond cleavage might lead to phosphorus impurities in palladium films formed from phosphine–palladium precursors but this work is the first to demonstrate the effect.[3c,7]

The thermolysis can be understood in terms of the mechanisms shown in Scheme 1, in which the reactions may occur either in the gas phase or, more probably adsorbed on the forming palladium surface. The palladium films are mostly smooth with few particles

Scheme 1. No Distinction Made between Gas Phase and Adsorbed State Species but Adsorbed State Mechanisms Probably Dominate in All Cases

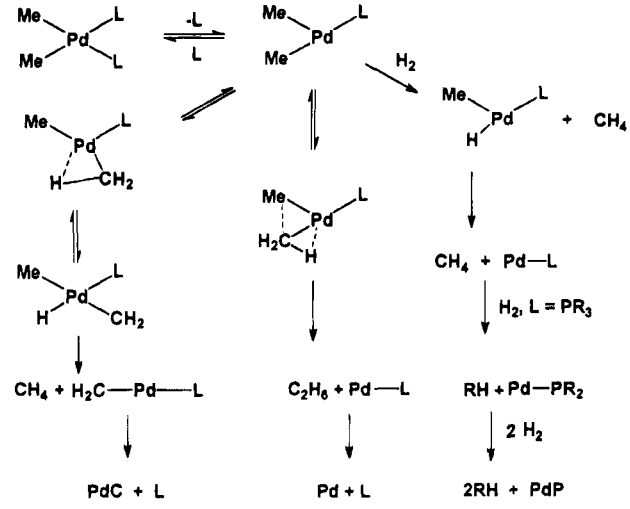

(Figure 2), and this is suggestive of a mechanism in which surface-catalyzed decomposition is dominant.

Under simple thermal CVD conditions, ethane is a major product, but its formation is inhibited in the presence of free ligand. It is likely that adsorbed-state steps dominate, but the mechanism of ethane formation shown in Scheme 1 is consistent with that proposed for solution phase thermolysis.[9,18,20–22] For related reductive eliminations from palladium(IV) and platinum(IV), it has been suggested that rocking of a methyl group to give an agostic CHM interaction, as indicated in the scheme, can rationalize the greater ease of elimination from the coordinatively unsaturated intermediate.[9,22] It is particularly significant that the thermolysis under CVD conditions of $[PdMe_2(tmeda)]$ leads to intramolecular reductive elimination. This was clearly demonstrated by the isotopic labeling experiment. There is an attractive mechanism in which dissociative absorption of the precursor on the forming palladium film leads to adsorbed methyl groups which can then migrate together and combine to form ethane. This would lead to formation of CH_3CD_3 from the mixed precursors $[PdMe_2(tmeda)]$ and $[Pd(CD_3)_2(tmeda)]$, but the crossover product was not observed (see Experimental Section). Thus, this surface methyl group coupling mechanism is disproved in this case. *When decomposition occurs from surface adsorbed precursor, the $PdMe_2$ groups must remain intact so that intramolecular coupling can occur.*

When thermolysis of *cis*-$[Pd(CD_3)_2L_2]$ yields CD_4, the α-elimination mechanism shown in the scheme is most reasonable, recognizing that this is likely to be an adsorbed-state process. However, it should be noted that methane formation is not retarded by free ligand nearly as greatly as is ethane formation, so it is not clear if the common intermediate $[PdMe_2L]$ shown in Scheme 1 is needed. Of course, the vacant site should facilitate the α-elimination step, but this might equally well occur within a surface adsorbed precursor molecule for which hydrogen migration from a methylpalladium group to

(19) Dryden, N.; Kumar.; R.; Ou, E.; Rashidi, M.; Roy, S.; Norton, P. R.; Puddephat, R. J.; Scott, J. D. *Chem. Mater.* **1991**, *3*, 675.

(20) See, for example: (a) Tatsumi, K.; Hoffmann, R.; Yamamoto, A.; Stille, J. K. *Bull. Chem. Soc. Jpn.* **1981**, *54*, 1857. (b) Low, J. J.; Goddard, W. A., III *J. Am. Chem. Soc.* **1986**, *108*, 6115.

(21) Stille, J. K., In *The Chemistry of the Carbon-Metal Bond*; Hartley, F. R., Patai, S., Eds.; John Wiley & Sons: Chichster, 1985; Vol. 2, Chapter 9, p 625.

(22) (a) Byers, P. K.; Canty, A. J.; Crespo, M.; Puddephatt, R. J.; Scott, J. D. *Organometallics* **1988**, *7*, 1363. (b) Roy, S.; Puddephatt, R. J.; Scott, J. D. *J. Chem. Soc., Dalton Trans.* **1989**, 2121.

the surface might occur instead. Once the CH_2Pd unit is formed, the carbon is probably destined to remain in the film and give rise to the observed carbon impurity, while the hydrogen atoms may undergo further migration reactions then combine with methylpalladium groups to give methane. In the presence of hydrogen, direct hydrogenolysis of methylpalladium groups to methane is clearly much faster than either reductive elimination or α-elimination pathways (this pathway is now shown in the scheme). Again this is probably a surface catalyzed reaction, and it leads to essentially carbon-free palladium films. There is little evidence on the nature of the steps which lead to phosphorus impurity in the films and only the overall process is shown in the scheme. The cleavage of P–C bonds is well-established in catalysis and often leads to deactivation of metal phosphine catalysts.[23] It is now shown to be a problem in CVD also.[3c,7]

(23) Garrou, P. G. *Chem. Rev.* **1985**, *85*, 171.

Conclusions

The dimethylpalladium(II) complexes are sufficiently volatile to act as CVD precursors for palladium films. However, they are not ideal since thermal CVD in the absence of a carrier gas leads to carbon impurities in the palladium films and hence to reduced conductivity and, interestingly, to observably higher Pd–Pd distances in the films compared to bulk palladium. Use of hydrogen carrier gas reduced the carbon impurity but led to phosphorus impurities in films prepared from $[PdMe_2(PR_3)_2]$. Mechanistic studies have shown that the carbon impurities are formed from methylpalladium groups and phosphorus impurities from the hydrogen-assisted decomposition of phosphine–palladium groups; it is probable that catalysis by the forming palladium surface dominates over simple gas-phase decomposition steps.

Acknowledgment. We thank the Ontario Centre for Materials Research (OCMR) and the NSERC (Canada) for financial support.